# Original Paper

## Leaching studies of soda–lime–silica glass using deuterium- and $^{18}O$-enriched solutions

Peter March[1]) and Friedrich Rauch
Institut für Kernphysik der Johann-Wolfgang-Goethe-Universität, Frankfurt am Main (FRG)

With a glass of composition (in mol%) 74 $SiO_2$, 16 $Na_2O$, 10 CaO, various leaching experiments were conducted, in which besides solutions of normal isotopic composition deuterium- and $^{18}O$-enriched solutions were used. The concentration profiles of deuterium, hydrogen, and $^{18}O$ in the sample were measured with nuclear analyzing techniques. A distinct H/D isotope effect was observed, showing that hydrogen takes part in the rate-determining step of leaching. The measured ratio of $^{18}O$ uptake to hydrogen uptake during leaching gives evidence for exchange of oxygen between the glass network and water molecules contained in the leached layer. From measurements on the exchange of hydrogen and oxygen between solution and leached layer, a high mobility of water molecules in the leached layer and evidence for condensation of silanol groups was found.

**Auslauguntersuchungen an Kalk–Natronsilicatglas mit deuterium- und $^{18}O$-angereicherten Lösungen**

Mit einem Glas der Zusammensetzung (Stoffmengenanteil in %) 74 $SiO_2$, 16 $Na_2O$, 10 CaO wurden Auslaugexperimente durchgeführt, in denen außer Lösungen mit normalen Isotopenverhältnissen auch deuterium- und $^{18}O$-angereicherte Lösungen benutzt wurden. Die Konzentrationsprofile von Deuterium, Wasserstoff und $^{18}O$ wurden mit kernphysikalischen Analysenmethoden bestimmt. Die Beobachtung eines ausgeprägten H/D-Isotopie-Effekts belegt, daß Wasserstoff am geschwindigkeitsbestimmenden Schritt der Auslaugung beteiligt ist. Das gemessene Verhältnis von $^{18}O$- zu Wasserstoff-Einlagerung gibt Hinweise auf den Austausch von Sauerstoff zwischen Glasnetzwerk und Wassermolekülen in der Auslaugschicht. Messungen zum Austausch von Wasserstoff und Sauerstoff zwischen Lösung und Auslaugschicht zeigen eine hohe Beweglichkeit von Wassermolekülen in der Auslaugschicht an und lassen auf die Kondensation von Silanolgruppen schließen.

### 1. Introduction

The leaching of alkali-containing silicate glasses by aqueous solutions has been investigated extensively for a long time because of its high technical and scientific significance. Great efforts have always been directed to understand the leaching mechanism. Some of the questions are: of what kind are the hydrogen-bearing water species entering the glass in conjunction with the loss of alkali, what is the rate-determining step in the growth of the leached layer, are there possible structural changes involving the glass network? In the past years much progress has been achieved and improved models have been developed, based on the results of specifically designed experiments employing a variety of analytical techniques, although a full (and generally accepted) theoretical description is still missing. For recent publications see e.g. [1 to 13]; overviews are given in [14 and 15] and contain more references on related work.

The aim of the present investigation was to obtain new or complementary information on some details of the leaching process by experiments with deuterium- and $^{18}O$-labelled solutions, using accelerator-based analyzing techniques for determining the concentration profiles of deuterium, hydrogen and $^{18}O$ in the surface layers of the glass samples. The experiments were done with a specific soda–lime–silica glass for which the leaching process was previously studied by measuring hydrogen and sodium concentration profiles [6]. This glass has also been used in leaching studies by Scholze [1] and Richter et al. [2], which allows interesting comparisons of the results. The present experiments were devised for clarifying three topics: the H/D isotope effect of the leaching rate, the ratio of oxygen uptake to hydrogen uptake during leaching, and the exchangeability of hydrogen and oxygen between solution and leached layer.

The extent to which the isotope effect occurs gives clues on the species involved in the rate-determining step. Previous work has yielded conflicting evidence on the existence of the effect: It was observed by Scholze et al. [16] and very recently by Pederson [8], but it was not found by Smets and Lommen [17] and by Richter et al. [2]. From the ratio of $^{18}O$ uptake to hydrogen uptake it was hoped to obtain information on the water species entering the glass and thus to allow a check of the conclusion drawn from the ratio of hydrogen uptake to sodium loss, H/Na, which is the more common basis for deducing the water species. For the glass under study it was found

Received 13 June 1989, revised manuscript 27 July 1989.
[1]) Now with: W. C. Heraeus GmbH, Hanau (FRG).

H/Na = 2.0 ± 0.3 [6]. This means that each hydrogen ion is accompanied by 0.5 $H_2O$ molecules, leading to an expected O/H ratio of 0.25. As it turned out, the measured ratio was much larger, giving evidence for another process connected with leaching. Measurements of the exchange rates of hydrogen isotopes and oxygen isotopes between a previously formed leached layer and a solution can give information on the chemical species in which the isotopes are transported and on the structure of the leached layer. A rather fast exchange for the hydrogen isotopes has been observed previously, using IR spectroscopy [1 and 14].

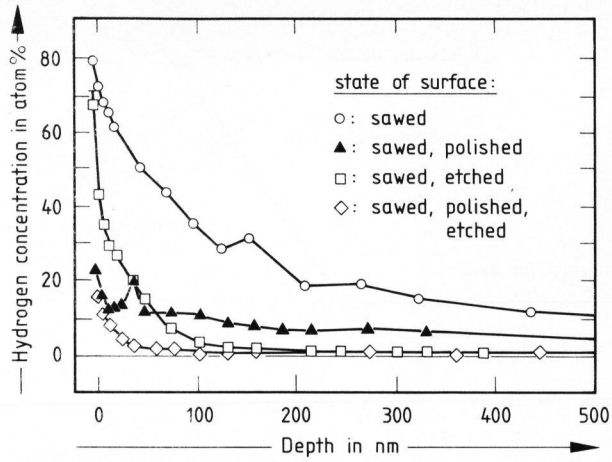


Figure 1. Hydrogen depth profiles of samples with different states of surface treatment.

## 2. Experimental procedure

### 2.1. Sample preparation

The glass used in the experiments had the composition (in mol%) 74 $SiO_2$, 16 $Na_2O$, 10 CaO. It was produced by melting the starting materials in a platinum crucible in a gas oven and then annealed at 550 °C. The glass slabs were cut in samples, (15 × 15 × 2) $mm^3$, and polished on one surface to optical quality. They were stored in a desiccator under vacuum. Before the start of an experiment, they were etched for 10 min in a solution of 0.5 % HF and 1 % $HNO_3$ in order to remove damaged, hydrated surface layers. The need for this treatment is obvious from figure 1 which displays hydrogen profiles (measured with the $^{15}N$ method described in section 2.2.) of differently treated samples. It is seen that after etching a polished sample only a thin, weakly hydrated layer remains.

Leached layers were produced at 90 °C for various leaching times, using acidic solutions in order to prevent network dissolution. The solutions were 1 n $H_2SO_4$, 1 n $D_2SO_4$ (99.8 % deuterium enrichment) and 0.5 n $H_2S^{18}O_4$ with 23 % $^{18}O$ enrichment. The $H_2SO_4$ leaching solution was contained in a borosilicate glass vessel, the surface-to-volume ratio (S/V ratio) was 3 $m^{-1}$. After removing the samples from the solution, they were rinsed with distilled water and with methanol. Thereafter, they were transferred into the vacuum chamber for the analyzing measurements. The leaching treatments with deuterium- and $^{18}O$-enriched solutions were performed in 7 $cm^3$ teflon beakers (S/V ratio = 56 $m^{-1}$). These were placed into the borosilicate vessel containing water at 90 °C. After the leaching treatment, the beakers were stored at −18 °C (1 h at most) until analysis could start. The samples were then removed from the solution and mounted on the target holder in the vacuum chamber without drying them; the chamber was then evacuated immediately. In this way, replacement of deuterium or $^{18}O$ by hydrogen or $^{16}O$ from exposure to air could be prevented. On the samples for the exchange experiments, at first leached layers of about 250 nm thickness were produced (1 n $H_2SO_4$, 90 °C, rinsing with distilled water and methanol). The samples were then placed for various times, at 23 °C, into $D_2O$ (99.8 % D) or $H_2{}^{18}O$ (21 % $^{18}O$) contained in teflon beakers (S/V ratio = 56 $m^{-1}$). At 23 °C, leaching and network dissolution can be neglected for the exchange times used. After the exchange treatment, the beakers were stored (1 h at most) until the analyzing measurements. The further sample handling was as described above.

### 2.2. Analyzing techniques

The measurements were performed in a vacuum chamber containing a rotatable target holder for up to 15 samples, a cold trap connected to a $LN_2$ (Liquid Nitrogen) vessel, and a heatable filament as electron emitter for preventing charging of the samples by the ion beam. The beam current was typically 30 nA; the beam spot was about (3 × 2) $mm^2$. The vacuum in the chamber was about $10^{-7}$ mbar. The ion beams were delivered by the Van de Graaff 7 and 2 MV accelerators of the Institut für Kernphysik, Frankfurt (FRG).

The measurements were carried out with the samples at room temperature. Test experiments showed that cooling the samples to prevent loss of hydrogen (water) in the vacuum was not necessary. In these experiments, the target holder was connected by copper wires to the cold trap so that the samples were cooled to below −100 °C when the $LN_2$ vessel was filled after evacuating the chamber. The hydrogen profiles obtained for these samples were the same as for uncooled samples. Furthermore, uncooled samples analyzed immediately after mounting them and evacuating the chamber (which took about 10 min) and analyzed again 10 h later showed no change in the hydrogen profiles.

For measuring the deuterium depth profiles and part of the hydrogen profiles, Elastic Recoil Detec-

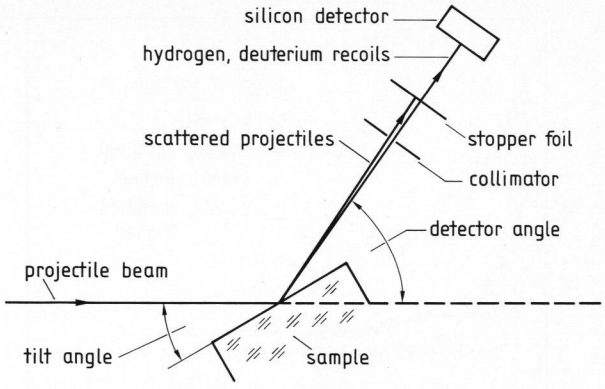


Figure 2. Schematic diagram illustrating the ERD technique.

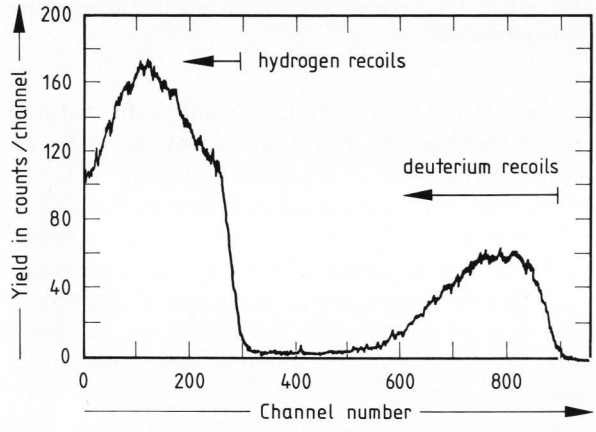


Figure 3. Example of an ERD spectrum, obtained for a sample of the H/D exchange experiments. The channel number is proportional to the recoil-ion energy.

tion (ERD) [18] was used. This technique is related to the better-known Rutherford backscattering (RBS) technique in that both rely on elastic scattering of fast (MeV) ions on target nuclei. While in RBS the scattered projectiles are detected and energy-analyzed, in ERD this is done for the target nuclei which have received momentum and kinetic energy in the scattering process and are recoiled into the forward hemisphere. The projectiles are chosen to be much heavier than the light elements or isotopes to be profiled. In the present measurements $^{40}$Ar ions of 20 MeV were used. The ERD technique is depicted schematically in figure 2. The sample is tilted with respect to the beam direction, so that recoils can leave the sample and reach the detector placed at a forward angle. In front of the detector a stopper foil is mounted, which prevents scattered projectiles and recoils of heavier elements comprising the sample from reaching the detector and deteriorating the spectra of the light recoils. This discrimination relies on the larger energy loss (stopping power) of heavier ions. The recoil energy $E_r$ is given by the following equation

$$E_r = 4\,E_p \cdot \cos^2\theta \cdot M_p\,M_r/(M_p + M_r)^2\,, \qquad (1)$$

where $E_p$ is the projectile energy, $\theta$ is the scattering angle and $M_r$ and $M_p$ are the recoil and projectile masses, respectively. One sees that hydrogen and deuterium recoils can be distinguished by their energies.

Recoils from the sample surface have energies given by equation (1) with $E_r$ equal to the bombarding energy. Recoils from scattering events inside the sample arrive at the detector with reduced energies, because the projectiles are slowed down before scattering as well as the recoils on their way out of the sample. This results in energy spectra for hydrogen and deuterium ions, which can be transformed into depth profiles using the known stopping power, $dE/dx$, of the sample and the cross sections for elastic scattering. A computer program was developed for performing this transformation. An example of a spectrum is shown in figure 3. The calibration for the ERD measurements, which involved basically the determination of the detector solid angle, was obtained from the analysis of samples whose hydrogen profiles were known from measurements with the $^{15}$N technique. From this procedure, the absolute accuracy of depth and concentration values and of total hydrogen and deuterium amounts is about 10 %. The relative uncertainties between different total amounts are below 5 %.

The depth resolution for ERD is limited by the detector resolution, the finite detector angle $\Delta\theta$ and by energy straggling in the sample and the stopper foil. In the measurements for this work it was 16 nm for hydrogen recoils and 23 nm for deuterium recoils, nearly independent of depth. The silicon detector was placed at 55°, at a distance of 127 mm from the sample. In front of the detector a tantalum diaphragm was placed with a 0.13 mm slit for defining $\Delta\theta$ and a 6.5 μm mylar stopper foil. The sample tilt angle was 27.5°.

Hydrogen depth profiles were partly measured with ERD and partly with Nuclear Reaction Analysis (NRA). The NRA technique employed is based on the resonance reaction $^1$H($^{15}$N, $\alpha\,\gamma$)$^{12}$C [19]. The presence of hydrogen is indicated by 4.43 MeV $\gamma$ radiation appearing when the sample under study is bombarded with $^{15}$N ions of sufficiently high energy. The $\gamma$ rays can be detected with a scintillation counter; in the measurements a 5″ × 5″ NaI detector positioned at 0° was employed.

Depth profiling relies on the fact that the reaction occurs only for projectiles of energy $E_r = 6.40$ MeV, which corresponds to a strong resonance in the reaction cross section. When the bombarding energy, $E_b$, is chosen as $E_r$, hydrogen at the sample surface is detected; when $E_b$ is raised, the reaction occurs at a certain depth at which the projectiles have lost sufficient energy to reach $E_r$. The depth $x$ is obtained from $x = (E_b - E_r)/(dE/dx)$, where $dE/dx$ is the stopping power of the sample. The number of $\gamma$ rays,

$N_\gamma$, at each energy is proportional to the local hydrogen concentration. Thus, by increasing $E_b$ stepwise and measuring $N_\gamma$ at each step, the hydrogen depth profile is obtained. The depth resolution of the $^{15}N$ measurements, 8 nm near the sample surface, is determined by the resonance width; it decreases slowly with depth due to energy straggling and is ≈30 nm at 400 nm depth. As calibration standard, required for determining the detector efficiency, a silicon wafer implanted with a known amount of hydrogen ions was used. The better depth resolution is an advantage compared with ERD; another one is that depth profiles are obtained directly and not from the transformation of the energy spectra. It cannot be applied to deuterium-containing samples, because a nuclear reaction between $^{15}N$ and deuterium produces a strong $\gamma$-ray background.

Profiling of $^{18}O$ was also performed with a NRA technique, utilizing the reaction $^{18}O(p, \alpha_0)^{15}N$ and especially the existence of a resonance at $E_r = 629$ keV [20]. The procedure of depth profiling is analogous to that of the $^{15}N$ technique. The number of $\alpha$ particles from the reaction of the protons at the resonance energy is measured as a function of the projectile energy, which is increased stepwise for sampling the $^{18}O$ concentration at increasing depths.

The $\alpha$ particles, which have an energy of about 3.4 MeV, were measured with a silicon detector placed at 135°; it was covered with a 1.3 μm aluminum foil in order to reduce the number of backscattered protons recorded by the detector. The depth resolution in these measurements was 23 nm at the sample surface and 31 nm at 300 nm depth. As calibration standard a silicon wafer implanted with a known amount of $^{18}O$ ions was used. The ensuing absolute accuracy of concentration and depth values was about 13 %. The relative uncertainty of individual profile points was between 5 and 15 %.

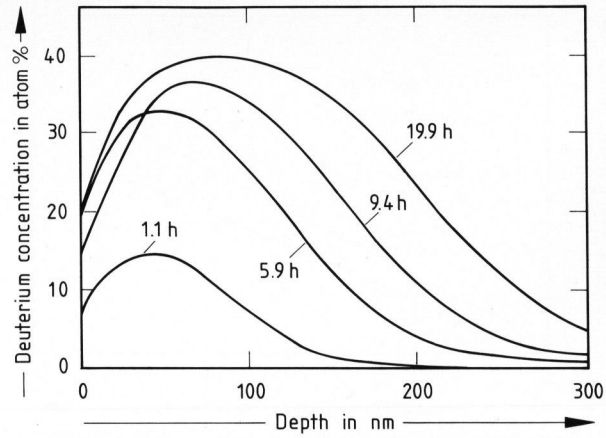


Figure 4. Deuterium depth profiles of samples leached at 90 °C in 1 n $D_2SO_4$ (99.8 % deuterium) for different leaching times.

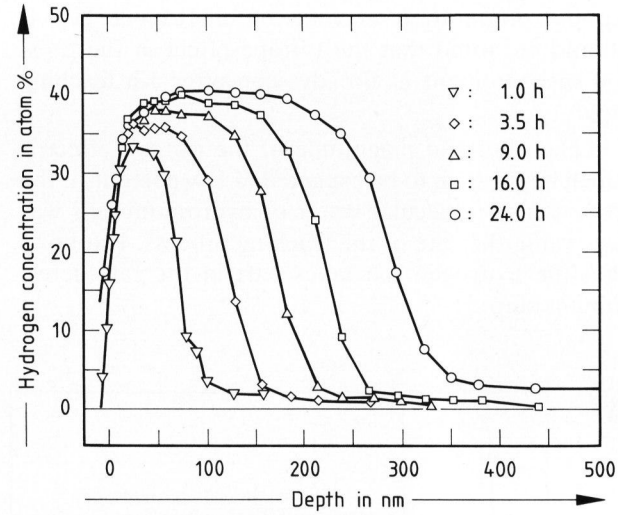


Figure 5. Hydrogen depth profiles of samples leached at 90 °C in 1 n $H_2SO_4$ for different leaching times.

## 3. Results and discussion

### 3.1. Isotope effect

The deuterium depth profiles obtained from samples leached in $D_2SO_4$ for different times are shown in figure 4. (The concentration values relate to a glass molecule $Si_1O_{2.35}Na_{0.43}Ca_{0.14}$.) These are to be compared to the hydrogen depth profiles displayed in figure 5 which were obtained for samples leached in $H_2SO_4$ [6]. (The difference in shape between the hydrogen and deuterium depth profiles is caused by the worse depth resolution of the ERD technique compared to the $^{15}N$ technique, which tends to smear out the profiles and to produce tails.) It is obvious that, for given leaching times, the width of the deuterium profiles, $\sigma(D)$, is smaller than that of the hydrogen profiles, $\sigma(H)$. A linear dependence on $\sqrt{t}$ is found for both $\sigma(D)$ and $\sigma(H)$, with $\sigma(H)$ increasing faster by a factor of $1.40 \pm 0.15$.

Another measure for the isotope effect is the total amount, $M$, of incorporated deuterium and hydrogen, respectively (figure 6). Both $M(D)$ and $M(H)$ show a linear dependence on $\sqrt{t}$, with $M(H)$ increasing faster by a factor of $1.25 \pm 0.13$.

These findings confirm the results of other authors on the existence of a H/D isotope effect. The reduction of the leaching rate determined in the present experiments is of similar magnitude as that observed by Scholze et al. [16], who found for a soda–lime–silica glass a 25 % difference of leached sodium between DCl and HCl solutions; furthermore, Pederson [8] found for a $Na_2O \cdot 3\,SiO_2$ glass that the amount of deuterium ions taken up into the glass from $D_2O$ was about 30 % smaller than the amount of hydrogen ions taken up from $H_2O$. Richter et al. [2] did not find an isotope effect in their short-time ($t \leq 1$ h) leaching experiments. This was interpreted as evidence that in the very beginning the leaching mechanism is different from that

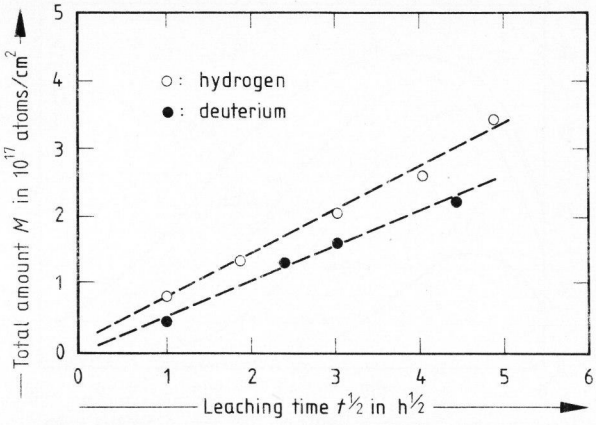


Figure 6. Total amounts of hydrogen and deuterium taken up during leaching as a function of the leaching time.

governing the following stages; also the special kind of sample preparation may be of importance [2]. It should be noted that the isotope effect in the present measurement is already seen after 1 h leaching time.

The observed magnitude of the isotope effect is much larger than to be expected (a few percent) if the diffusion of molecular water or hydronium ions was governing the rate of the leaching process. It follows that the hydrogen ion takes part in the rate-determining step.

As to the nature of this step, diffusion of hydrogen ions can probably be excluded, because bare hydrogen ions should not exist in the leached layer and rather be bonded to water molecules, forming hydronium ions during their movement through the leached layer [15 and 21]. Pederson [8] has proposed a model based on transition-state theory which involves a ≡Si−O−Si≡ group and a hydronium ion, with the hydrogen ion near the network oxygen and the water oxygen near one silicon. The rate-determining step is the breaking of a H−O bond (or a D−O bond) of the water molecule, which together with the breaking of the Si−O bond leads to two SiOH groups and an $H^+$ ion. The ensuing hydrolysis is assumed to be a necessary precursor for $Na^+ \leftrightarrow H^+$ exchange. While this model explains the observed isotope effect, it may need further experimental scrutinizing. It is, however, consistent with the observation of high mobility of water molecules in the leached layer (see section 3.3.) which should also hold for hydronium ions and which places the location of the rate-determining step at the boundary zone between leached layer and bulk glass.

For later use it is noted that the rate constant $k$ describing the movement of that boundary has the value $k \approx 6 \cdot 10^{-15}$ cm$^2$/s (at 90 °C), as derived from the experimentally found dependence $\sigma^2 = k\,t$.

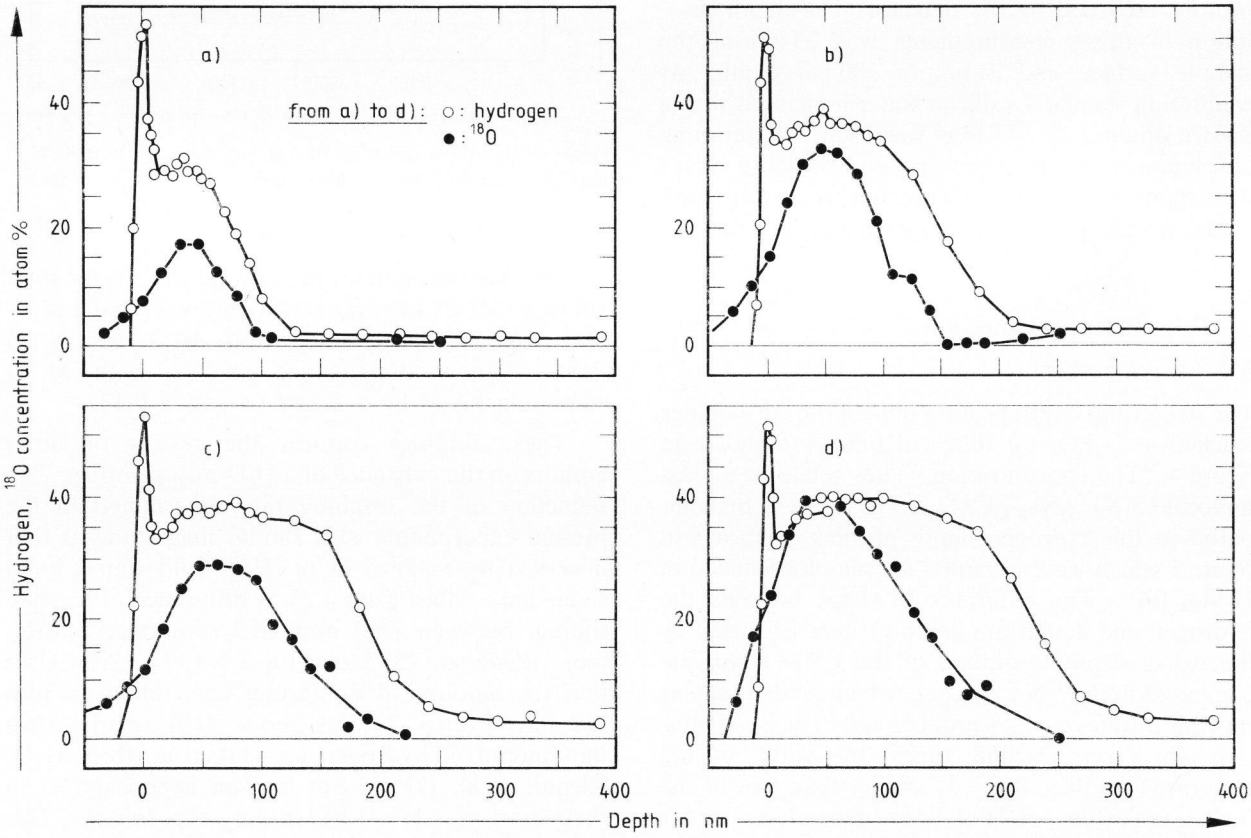


Figures 7a to d. Hydrogen and $^{18}O$ depth profiles of samples leached at 90 °C in 0.5 n $H_2S^{18}O_4$ (23 % $^{18}O$) for different leaching times, a) 1 h, b) 5.9 h, c) 10 h, d) 15.9 h.

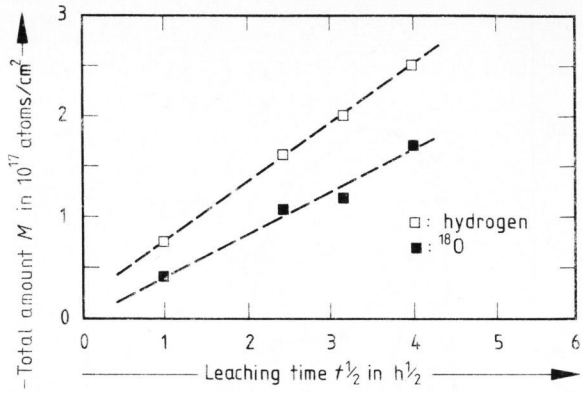


Figure 8. Total amounts of hydrogen and $^{18}O$ taken up during leaching as a function of the leaching time.

### 3.2. $^{18}O/H$ uptake ratio

Measurements of the uptake ratio $^{18}O/H$ were performed on samples leached between 1 and 25 h. It turned out that $^{18}O$ was incorporated in conveniently measurable amounts. The hydrogen and $^{18}O$ profiles of these samples are displayed in figures 7a to d. (The narrow peak at zero depth in the hydrogen profiles arises from adsorbed hydrocarbons due to bad vacuum during these hydrogen profiling measurements; this peak was subtracted in determining the integral amount of hydrogen.) It is seen that $^{18}O$ uptake increases with leaching time, roughly in parallel to hydrogen uptake. The total amounts $M(^{18}O)$ and $M(H)$ are plotted in figure 8. Like $M(H)$ also $M(^{18}O)$ shows a linear dependence on $\sqrt{t}$. The $^{18}O/H$ ratio increases slightly from 0.53 to 0.67, with an average value of 0.61.

These values are ten times higher than the value 0.06 which follows from the H/Na ratio (see section 1.) and the incomplete (23 %) $^{18}O$ enrichment of the leaching solution. This implies that besides $H^+ \leftrightarrow Na^+$ ion exchange and indiffusion of water a further process is connected with leaching. Most likely, this process is incorporation of $^{18}O$ into the glass network, with the following (reversible) chain of reactions:

$$\equiv Si-{}^{16}O-Si\equiv + H_2{}^{18}O \rightarrow \equiv Si-{}^{18}OH + H{}^{16}O-Si\equiv \rightarrow \equiv Si-{}^{18}O-Si\equiv + H_2{}^{16}O\,. \quad (2)$$

(Similar reactions involving the oxygen bonded with calcium and sodium will also occur.)

These reactions have previously been invoked to account for the results of experiments on the reaction of vitreous silica with steam at high temperatures [22]. In a recent paper, Pederson et al. [7] reported similar results; in long-term leaching experiments with a 4-component silicate glass they found for the total amounts of $^{18}O$ and deuterium (related to isotopic enrichments of 100 %) the ratio $^{18}O/D = 1.6$ and used the reactions of equation (2) to explain this observation.

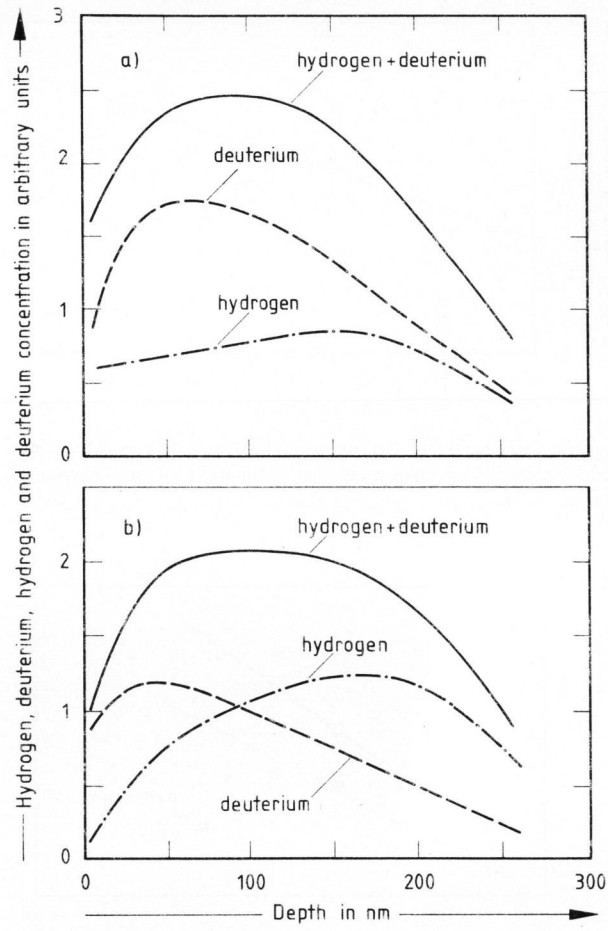


Figures 9a and b. Hydrogen and deuterium depth profiles and summed profiles of samples from the H/D exchange experiments for two exchange times, a) $t_e = 5$ h, b) $t_e = 29$ h.

A detailed comparison of the $^{18}O$ and hydrogen profiles in figures 7a to d provides additional evidence for the incorporation of $^{18}O$ into the network. The width of the $^{18}O$ profiles is smaller than that of the hydrogen profiles, the difference becoming larger with extended leaching time. On the other hand, the ratio of maximum $^{18}O$ concentration to maximum hydrogen concentration increases with $t$. Both observations are in accordance with the reaction chain of equation (2): $^{18}O$-labelled water molecules indiffusing from the solution will on the average loose their $^{18}O$ atom to the network and $^{16}O$-containing molecules will penetrate more deeply, so that the strongest $^{18}O$ enrichment is near the surface. The transfer of $^{18}O$ to the network will be more frequent than pickup by unlabelled water molecules until the $^{18}O/^{16}O$ ratio in the network equals that of the solution. In the experiments this equilibrium (0.3) has not been reached. The highest $^{18}O$ concentration of 40 %, corrected for the $^{18}O$ fraction bound in water molecules, corresponds to 0.36 $^{18}O$ atoms per silicon atom and to a $^{18}O/^{16}O$ ratio in the network of 0.18.

The difference in width of the $^{18}O$ and hydrogen profiles found in this study was not observed in

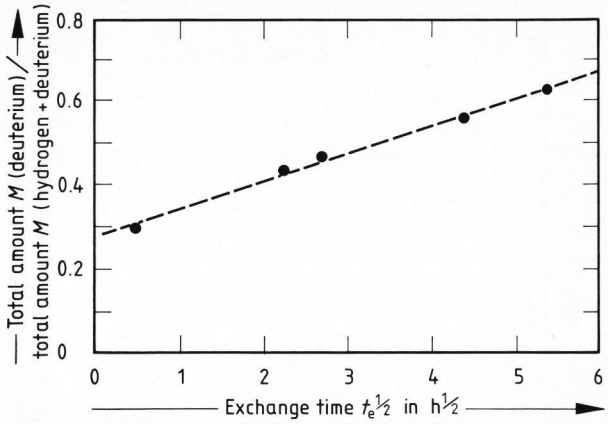


Figure 10. Fraction of hydrogen in the leached layer which has been replaced by deuterium as a function of the exchange time $t_e$.

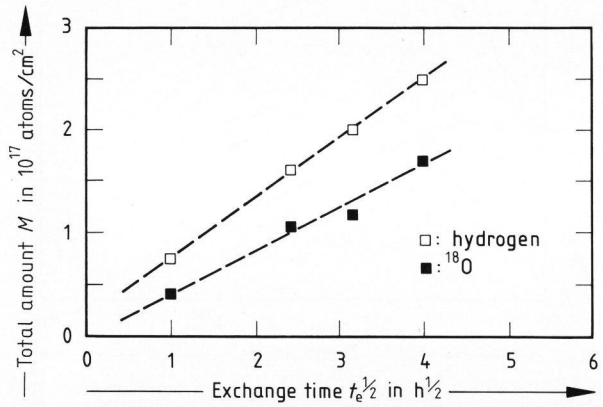


Figure 12. Total amounts of deuterium and $^{18}O$ taken up as a function of the exchange time.

short-term leaching experiments [9]; the reason is probably the same as for the nonobservation of the isotope effect (see section 3.1.).

### 3.3. Isotope exchange between leached layer and solution

For the H/D exchange experiments, both the profiles of deuterium uptake from exchange of hydrogen and the profiles of the remaining hydrogen were measured. Profiles for two exchange times $t_e$ are shown in figures 9a and b; also shown is the sum of both isotope concentrations, which agrees well with the original hydrogen profile. It can be seen how deuterium replaces hydrogen throughout the whole layer, in an amount which increases with $t_e$. The exchanged fraction D/(H+D) is plotted in figure 10. About 1/3 of the hydrogen is replaced rather fast, then the exchange proceeds slower, following a $\sqrt{t}$ law. The longest exchange time in the experiments was not sufficient to allow complete exchange, but about 65 % of the hydrogen has been replaced and the curve through the data points does not indicate saturation; this will be dealt with later in this section.

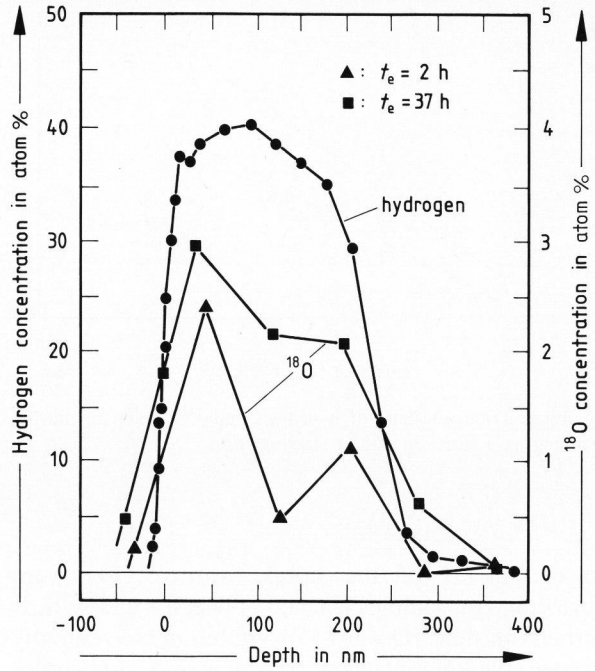


Figure 11. $^{18}O$ depth profiles of two samples from the $^{16}O/^{18}O$ exchange experiments for two different exchange times and the hydrogen profile of one of the samples which is nearly identical with the hydrogen profiles of all the investigated samples.

A very similar behavior as for deuterium uptake due to H/D exchange was found for $^{18}O$ uptake due to $^{16}O/^{18}O$ exchange. Figure 11 shows two of the $^{18}O$ profiles and for comparison the hydrogen profile of one of the samples (the hydrogen profiles of all the samples are nearly identical). Like deuterium also $^{18}O$ penetrates rather fast through the whole leached layer, and then the concentration increases at all depths.

It should be noted that the widths of the $^{18}O$ and deuterium profiles, even for the longest exchange times, do not exceed the width of the original hydrogen profile. This is in accordance with the expectation that the thickness of the leached layer does not increase during the exchange experiments conducted at 25 °C. From the activation energy for the increase of the leached layer of 80 kJ/mol, which has been determined in separate measurements, it follows that the layer grows 500 times more slowly at 25 than at 90 °C, with a rate of about $10^{-17}$ $cm^2/s$. Furthermore, $^{18}O$ uptake into the glass network can very likely be neglected at this lower temperature; it would be significant only if this process had a much smaller activation energy.

The total amounts of $^{18}O$, normalized to 100 % $^{18}O$ enrichment of the exchange bath, are compared in figure 12 with the total amounts of deuterium for the different exchange times. Both quantities have the same time behavior, with a fast increase at the beginning and a slower one with a $\sqrt{t}$ dependence for the following period. Most significant is that the (average) ratio of $M(D)/M(^{18}O)$ of 1.9 ± 0.2 is very close to 2, thus giving strong support to the

expectation of both isotopes being transported in water molecules.

From the $^{18}O$ and deuterium amounts taken up, one can deduce diffusion coefficients $D$, using the relation $D = \pi M^2/4\, C_0^2\, t$, where $C_0$ is the surface concentration. Because $C_0$ is not well-defined in the profiles, the uncertainty for $D$ is about 40 %. The $D$ values for both isotopes are very similar; at the beginning $D \approx 2 \cdot 10^{-14}$ cm$^2$/s, and for $t_e > 2$ h, $D \approx 3 \cdot 10^{-15}$ cm$^2$/s.

These values are about three orders of magnitude larger than the rate constant for leaching at 25 °C. In other words, the mobility of water in the leached layer is rather high and does certainly not limit the rate of leaching. A high mobility of water in the leached layer has also been observed by Scholze [14] in exchange experiments with $D_2O$, using IR spectroscopy. For a glass of the composition (in mol%) 74 $SiO_2$, 20 $Na_2O$, 6 CaO, the diffusion coefficient for replacement of $H_2O$ in the leached layer by $D_2O$ from $D_2O$ water was found as $D = 2 \cdot 10^{-12}$ cm$^2$/s.

From the absolute value of $M$(D) further information can be inferred. As noted above, at least 65 % of the hydrogen in the leached layer has been replaced by deuterium and a higher degree of exchange for larger $t_e$ values seems likely. This means that distinctly more hydrogen is bound in water molecules than the fraction 50 % incorporated during leaching.

The higher degree of exchangeable hydrogen can be explained by assuming that ≡Si–OH groups arising from $H^+ \leftrightarrow Na^+$ ion exchange at least partly condensate according to the reaction:

$$\equiv Si-OH + HO-Si\equiv \rightarrow \equiv Si-O-Si\equiv + H_2O \quad (3)$$

so that new water molecules are formed. This condensation reaction has previously been proposed [1] to explain the observation obtained by IR spectroscopy that almost 100 % of the hydrogen in the leached layer is bound in water molecules.

As has been discussed before [14], the condensation leads to a change in the structure of the glass network which involves a phase separation [23]. While this changed structure is likely to enhance the mobility of water in general it may also be that a part of the water is more mobile than the rest, e.g. water molecules agglomerated in tiny "pools" as compared to isolated water molecules in the network. The fast penetration of deuterium and $^{18}O$ through the whole leached layer at the beginning of the exchange treatment and the large diffusion coefficient for the first stage are interpreted as indicative for such a partition.

## 4. Summary and conclusion

Leaching experiments on a soda–lime–silica glass with $^{18}O$- and deuterium-enriched solutions have been performed and the resulting concentration profiles of $^{18}O$, deuterium and hydrogen have been determined with nuclear analyzing techniques. Valuable information on several aspects of the leaching process could be deduced from the experimental results. This process is found to be of rather complex nature.

From measurements of the leaching rates in deuterium-enriched and normal solutions, the existence of an H/D isotope effect was confirmed. The conclusion to be drawn is that the hydrogen ion takes part in the rate-determining step of the leaching process.

Measurements on the rate of exchange of deuterium and $^{18}O$ from a solution against hydrogen and $^{18}O$ from a leached layer showed a high mobility of water molecules in the layer, with the rate of $H_2O$ transport being much higher than the leaching rate. From the amount of hydrogen exchangeable between the leached layer and the bordering solution it could be concluded that ≡Si–OH groups arising from $H^+ \leftrightarrow Na^+$ ion exchange at least partly condensate to ≡Si–O–Si≡ and $H_2O$, thus forming a restructured glass network.

The measurements on the amount of $^{18}O$ uptake from an isotopically labelled leaching solution led to the result that there is a strong exchange of oxygen between the glass network and water molecules in the leached layer. This process has to be incorporated in an improved theoretical description of glass leaching, besides $H^+ \leftrightarrow Na^+$ ion exchange and indiffusion of water.

So far the experimental information on this oxygen-exchange process is rather limited, and its detailed investigation may become a new, rich field of studies on glass leaching. Such studies should include extended measurements of the relation between $^{18}O$ and hydrogen depth distributions and their time development, measurements on the extent of exchange when the sample is not in contact with a solution, and on the temperature dependence of the exchange process; of course the dependence on the glass composition will also help for a deeper understanding.

*

The authors are indebted to Prof. H. Scholze for interesting discussions. They would like to thank him and Dr. R. Conradt for providing polished glass samples. This work was supported by the Deutsche Forschungsgemeinschaft, Bonn-Bad Godesberg (FRG).

## 5. References

[1] Scholze, H.: Bedeutung der ausgelaugten Schicht für die chemische Beständigkeit: Untersuchungen an einem Kalk-Natronsilicatglas. Glastech. Ber. **58** (1985) no. 5, p. 116–124.

[2] Richter, T.; Frischat, G. H.; Borchardt, G.: Short-time leaching of a soda–lime glass in $H_2O$ and $D_2O$. Phys. Chem. Glasses **26** (1985) no. 6, p. 208–212.
[3] Schäfer, J.; Schaeffer, H. A.: Leaching of alkali silicate glasses – formation of hydrated layers, surface and diffusion-controlled kinetics. Riv. Stn. Sper. Vetro **14** (1984) no. 5, p. 79–82.
[4] Bunker, B. C.; Arnold, G. W.; Beauchamp, E. K. et al.: Mechanisms for alkali leaching in mixed-Na-K silicate glasses. J. Non-Cryst. Solids **58** (1983) no. 2/3, p. 295–322.
[5] Doremus, R. H.; Mehrotra, Y.; Lanford, W. A. et al.: Reaction of water with glass: influence of a transformed surface layer. J. Mater. Sci. **18** (1983) p. 612–622.
[6] March, P.; Rauch, F.: Hydration of soda-lime glasses studied by ion-induced nuclear reactions. Nucl. Instrum. Methods **B15** (1986) p. 516–519.
[7] Pederson, L. R.; Baer, D. R.; McVay, G. L. et al.: Reaction of soda lime silicate glass in isotopically labelled water. J. Non-Cryst. Solids **86** (1986) p. 368–380.
[8] Pederson, L. R.: Comparison of sodium leaching rates from a $Na_2O \cdot 3SiO_2$ glass in $H_2O$ and $D_2O$. Phys. Chem. Glasses **28** (1987) no. 1, p. 17–21.
[9] Frischat, G. H.; Richter, T.; Borchardt, G. et al.: Surface analysis of a glass leached with stable isotopes. Microchim. Acta [Wien] 1987, I, p. 179–192.
[10] Dran, J.-C.; Della Mea, G.; Paccagnella, A. et al.: The aqueous dissolution of alkali silicate glasses: reappraisal of mechanisms by H and Na depth profiling with high energy ion beams. Phys. Chem. Glasses **29** (1988) no. 6, p. 249–255.
[11] Belyustin, A. A.; Shul'ts, M. M.: Interdiffusion of cations and the accompanying processes in the surface layers of alkali silicate glasses treated with aqueous solutions. Sov. J. Glass Phys. Chem. **9** (1983) no. 1, p. 1–24.
[12] Bunker, B. C.; Tallant, D. R.; Headley, T. J. et al.: The structure of leached borosilicate glass. Phys. Chem. Glasses **29** (1988) no. 3, p. 106–120.
[13] Schnatter, K. H.; Doremus, R. H.; Lanford, W. A.: Hydrogen analysis of soda-lime silicate glass. J. Non-Cryst. Solids **102** (1988) p. 11–18.
[14] Scholze, H.: Glass-water interactions. J. Non-Cryst. Solids **102** (1988) p. 1–10.
[15] Ernsberger, F. M.: Current theories of glass durability. In: XIV International Congress on Glass, New Delhi 1986. Coll. papers. Vol. 2. Calcutta: Indian Ceramic Society 1986. p. 319–326.
[16] Scholze, H.; Helmreich, D.; Bakardjiev, I.: Untersuchungen über das Verhalten von Kalk-Natrongläsern in verdünnten Säuren. Glastech. Ber. **48** (1975) no. 12, p. 237–247.
[17] Smets, B. M. J.; Lommen, T. P. A.: The leaching of sodium containing glasses: ion exchange or diffusion of molecular water? J. Phys. **43** (1982) Colloq. C9, p. C9-649–C9-652.
[18] L'Ecuyer, J.; Brassard, C.; Cardinal, C. et al.: The use of $^6Li$ and $^{35}Cl$ ion beams in surface analysis. Nucl. Instrum. Methods **149** (1978) p. 271–277.
[19] Lanford, W. A.; Trautvetter, H. P.; Ziegler, J. F. et al.: New precision technique for measuring the concentration versus depth of hydrogen in solids. Appl. Phys. Lett. **28** (1976) no. 9, p. 566–568.
[20] Rosencher, E.; Straboni, A.; Rigo, S. et al.: An $^{18}O$ study of the thermal oxidation of silicon in oxygen. Appl. Phys. Lett. **34** (1979) no. 4, p. 254–256.
[21] Ernsberger, F. M.; The role of molecular water in the diffusive transport of protons in glass. Phys. Chem. Glasses **21** (1980) no. 4, p. 146–149.
[22] Roberts, G. J.; Roberts, J. P.: An oxygen tracer investigation of the diffusion of 'water' in silica glass. Phys. Chem. Glasses **7** (1966) no. 3, p. 82–89.
[23] Tomozawa, M.; Capella, S.: Microstructure in hydrated silicate glasses. J. Am. Ceram. Soc. **66** (1983) no. 2, p. C-24–C-25.

90R0516

## Correction

P. March and F. Rauch: Leaching studies of soda–lime–silica glass using deuterium- and $^{18}O$-enriched solutions. Glastech. Ber. **63** (1990) no. 6, p. 154–162.

In figures 9a and b (p. 159) of the cited paper the exchange times have been mixed up, i.e. figure 9a stands for an exchange time of 29, figure 9b for one of 5 h. Moreover, on p. 160 a wrong diagram has been published as figure 12. The correct presentation including caption is shown as follows:

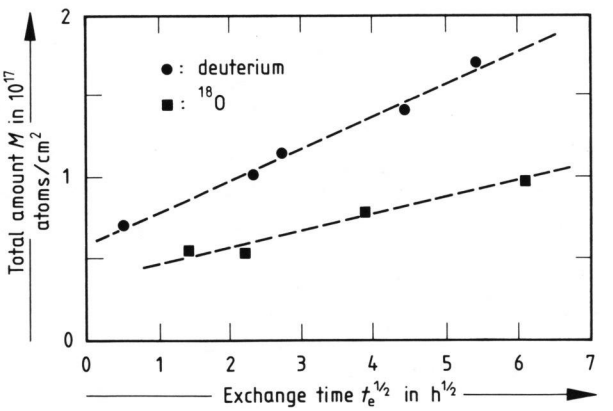


Figure 12. Total amounts of deuterium and $^{18}O$ taken up as a function of the exchange time.